Applied Surface Science 555 (2021) 149586

Contents lists available at ScienceDirect

Applied Surface Science

journal homepage: www.elsevier.com/locate/apsusc

Full Length Article

Two-dimensional closely-packed gold nanoislands: A platform for optical data storage and carbon dot generation☆

Peitao Wen [a], Yi Xu [b], Shulei Li [a], Zhibo Sun [a], Mingcheng Panmai [a], Jin Xiang [c,*], Shaolong Tie [d], Sheng Lan [a,**]

[a] Guangdong Provincial Key Laboratory of Nanophotonic Functional Materials and Devices, School of Information and Optoelectronic Science and Engineering, South China Normal University, Guangzhou 510006, China
[b] Department of Electronic Engineering, College of Information Science and Technology, Jinan University, Guangzhou 510632, China
[c] Department of Electrical and Computer Engineering, University of Wisconsin-Madison, Madison, WI 53705, USA
[d] School of Chemistry, South China Normal University, Guangzhou 510006, China

ARTICLE INFO

Keywords:
Optical data storage
Carbon dot
Au nanoparticle
Femtosecond laser pulse

ABSTRACT

Polymer films doped with gold (Au) nanoparticles have been successfully employed to realize optical data storage and carbon dot generation. However, such nanomaterials are not expected to have a long lifetime because polymers are not stable against humidity and heat. Here, we propose the use of two-dimensional closely-packed Au nanoparticles deposited on a silica substrate as the platform for realizing simultaneously high-density optical data storage and efficient carbon dot storage. The hot spots formed by plasmonic coupling between Au nanoparticles enable the realization of polarization and wavelength multiplexing in optical data storage with high quality and low energy. In addition, strongly localized temperature distribution can be achieved in closely-packed Au nanoparticles exploited to produce luminescent carbon quantum dots by using direct laser writing. Our findings indicate the potential applications of this new nanomaterial in the fabrication of novel photonic devices for optical data storage, optical display, and optical sensing in the future.

1. Introduction

Nanoparticles of noble metals, such as gold (Au) nanoparticles of different shapes, have attracted great interest in the last two decades due to the existence of surface plasmon resonances (SPRs) which exhibit potential applications in the fields of plasmonics [1], nanophotonics [1–8] and biophotonics [1,9]. The SPRs of spherical Au nanoparticles generally appear at ~ 530 nm while cylindrical (or rod-like) Au nanoparticles support another SPR located at a longer wavelength, usually in the near infrared spectral range [10,11]. SPRs can also be created in the assemblies of Au nanoparticles of different fashions, such as dimers, oligomers and closely-packed nanoparticle arrays. It has been known that photoluminescence (PL) can be generated by resonantly exciting the SPRs of single Au nanoparticles or assemblies of Au nanoparticles by using either continuous wave or pulsed lasers [3,12,13]. Apart from down-converted PL which is generally observed in Au nanoparticles excited by continuous wave lasers, up-converted PL can also be generated when Au nanoparticles are excited by pulsed lasers. The up-converted PL of Au nanoparticles (e.g., Au nanorods) generated by femtosecond laser pulses, which is commonly referred to as two-photon-induced luminescence (TPL), has received intensive and extensive studies in the past decades owing to its potential applications in bio-imaging [14], photothermal therapy [15] and optical data storage [16–19]. Although the physical mechanism for the TPL of Au nanorods remains controversial, it is now gradually accepted that the luminescence emitting from Au nanoparticles belongs to hot-electron intraband luminescence (HEIL) [20–23]. The HEIL from Au nanoparticles exhibits a broad spectrum spanning the visible to near infrared spectral range. Also, the slope extracted from the dependence of the luminescence intensity on the excitation irradiance in a logarithmic coordinate is proportional to the energy of the emitting photons.

In an assembly of Au nanoparticles, plasmonic coupling may occur when the volume density of Au nanoparticles is sufficiently large. In this case, hot spots with significantly enhanced electric fields are created in

☆ Fully documented templates are available in the elsarticle package on http://www.ctan.org/tex-archive/macros/latex/contrib/elsarticleCTAN

* Corresponding author.
** Corresponding author.
E-mail addresses: jxiang29@wisc.edu (J. Xiang), slan@scnu.edu.cn (S. Lan).

https://doi.org/10.1016/j.apsusc.2021.149586
Received 4 January 2021; Received in revised form 1 March 2021; Accepted 15 March 2021
Available online 2 April 2021

the gap regions between Au nanoparticles. As a result, the linear and nonlinear absorptions of the assembly are governed by these hot spots (or the Au nanoparticles adjacent to the hot spots). It has been confirmed that the plasmonic coupling between Au nanoparticles can be exploited to enhance both the linear and nonlinear optical responses of the assembly, including HEIL [20]. Since the hot spots are strongly correlated with the gap widths between Au nanoparticles, they can be eliminated through the thermal reshaping of Au nanoparticles induced by femtosecond laser pulses, quenching the HEIL from the assembly. Recently, the polarization and wavelength sensitive hot spots have been exploited to realize optical data storage with ultrahigh density and ultralow energy [16–18].

Apart from the strong localization of electric field, the plasmonic coupling between Au nanoparticles is also important in the achievement of highly localized temperature distribution. It was found that a Fano resonance, which is formed by the plasmonic coupling between Au nanoparticles, can be generated in the extinction spectrum of an oligomer of Au nanoparticles [24]. A spatially localized temperature distribution can be realized when the Fano resonance is resonantly excited. The highly localized temperature distribution, together with the catalytic properties of Au nanoparticles, leads to the formation of carbon quantum dots with efficient emission in the visible light spectrum in a polymer film doped with Au nanoparticles [24].

So far, the materials used for optical data storage and carbon dot generation are thin polymer films heavily doped with Au nanoparticles [3,12,16,24]. Since Au nanoparticles are embedded in a polymer matrix, any deformation in the supporting polymer may significantly affect the distance between Au nanoparticles and the plasmonic coupling between them. As compared with dielectric materials, polymers are not stable against to humidity and temperature. The adsorption of water vapor in the atmosphere may lead to the deformation or even melting of polymer films. During data recording, the heat released from Au nanoparticles can also result in the deformation, modification and even dehydration of the polymer, as evidenced in the generation of carbon quantum dots [24–26]. Therefore, the data storage media made of polymers films, which are not expected to have a long lifetime, are not satisfied for practical applications. From the viewpoint of carbon dot generation [25–29], the wavelength range in which the Fano resonances are available for creating small carbon dots, is limited to 600–650 nm. This wavelength window is narrow and incompatible with the commonly used femtosecond laser source (~ 800 nm). Therefore, a new material platform on which optical data storage and carbon dot generation can be simultaneously implemented is highly desirable.

In this article, we proposed a simple platform, which comprises two-dimensional closely-packed Au nanoislands deposited on a silica (SiO_2) substrate, for simultaneously realizing high-quality optical data storage and efficient carbon dot generation. We confirmed by numerical simulation that polarization and wavelength-sensitive hot spots are present in the closely-packed Au nanoislands and demonstrated that high-quality optical data storage with polarization multiplexing can be realized by using femtosecond laser pulses. We also revealed that spatially localized temperature distribution can be achieved in closely-packed Au nanoislands after the irradiation of femtosecond laser pulses and demonstrated the generation of carbon dots emitting white light efficiently. We compared the efficiencies of carbon dot generation in different polymers including polyvinyl alcohol (PVA), polymethyl methacrylate (PMMA) and polyvinyl pyrrolidone (PVP) and found that PVP is the best one in producing highly luminescent carbon dots.

2. Results and discussion

Closely-packed Au nanoislands used in this work were obtained by sputtering Au on a SiO_2 substrate. The morphology of Au nanoislands deposited on the SiO_2 substrate depends strongly on the sputtering time (t), as shown in Fig. 1a-f where the transmission electron microscopy (TEM) images of Au nanoislands obtained by using different sputtering times are presented. It can be seen that Au nanoislands become closely-packed for a sputtering time longer than 15 s. With increasing sputtering time, more and more small Au nanoislands are merged into larger nanoislands and the gaps between nanoislands become narrower. If the sputtering time is further increased, it is expected that all the Au nanoislands will eventually disappear and a flat Au film will be obtained. In Fig. 1g, we present the TEM image of a single Au nanoparticle from which the crystalline structure of the Au nanoparticle can be identified. It can be seen that the Au nanoparticle is a polycrystalline, which is further confirmed by the eletron diffraction pattern shown in Fig. 1h.

In order to gain a deep insight into the morphology change of Au nanoislands with increasing sputtering time, we have analyzed the size distributions of Au nanoislands obtained at different sputtering times by using a software with which the areas of all Au nanoislands in the SEM images can be extracted, as shown in Fig. 2. It can be seen that the average size (or area) of Au nanoislands increases rapidly with increasing sputtering time, implying the merge of small Au nanoislands into large ones. In addition, it is noticed that the size distribution also becomes larger at the same time. More importantly, it is remarkable that the filling ratio of Au nanoislands increases also rapidly from ~ 52% at t = 10 s to ~ 77% at t = 40 s (or the decrease of the space filling ration from ~ 48% to ~ 23%), implying reduction in the gap width between Au nanoislands that leads to the formation of plasmonic hot spots.

As discussed at the begining, Au nanoparticles can emit efficient HEIL if the SPRs of Au nanoparticles are resonantly excited by using femtosecond laser pulses. A well-known case is Au nanorods with longitudinal SPRs appearing in the near infrared spectral range [3,13]. Efficient HEIL from Au nanorods has been applied in bioimaging, photothermal therapy and optical data storage [15,19]. Isolated Au nanoparticles with sperical shapes do not emit HEIL under the excitation of 800-nm femtosecond laser pulses because their SPRs appear at ~ 530 nm [3]. However, a dimer of spherical Au nanoparticles may have its SPR appear in near infrared spectral range, depending on the gap between the two constituent Au nanoparticles [30]. In this case, a plasmonic hot spot is created in the gap region of the dimer and it can emit efficient HEIL under the excitation of femtosecond laser pulses. By inspecting the morphology of closely-packed Au nanoislands, one can

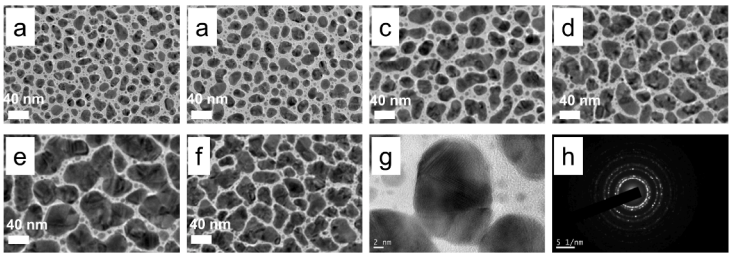

Fig. 1. TEM images of the two-dimensional Au nanoislands obtained by using different sputtering times of (a) 10 s, (b) 15 s, (c) 20 s, (d) 25 s, (e) 30 s, and (f) 40 s. The magnified image for a single Au nanoparicle and the corresponding electron diffraction pattern showing the crystalline structure of the Au nanoparticle are shown in (g) and (h), respectively.

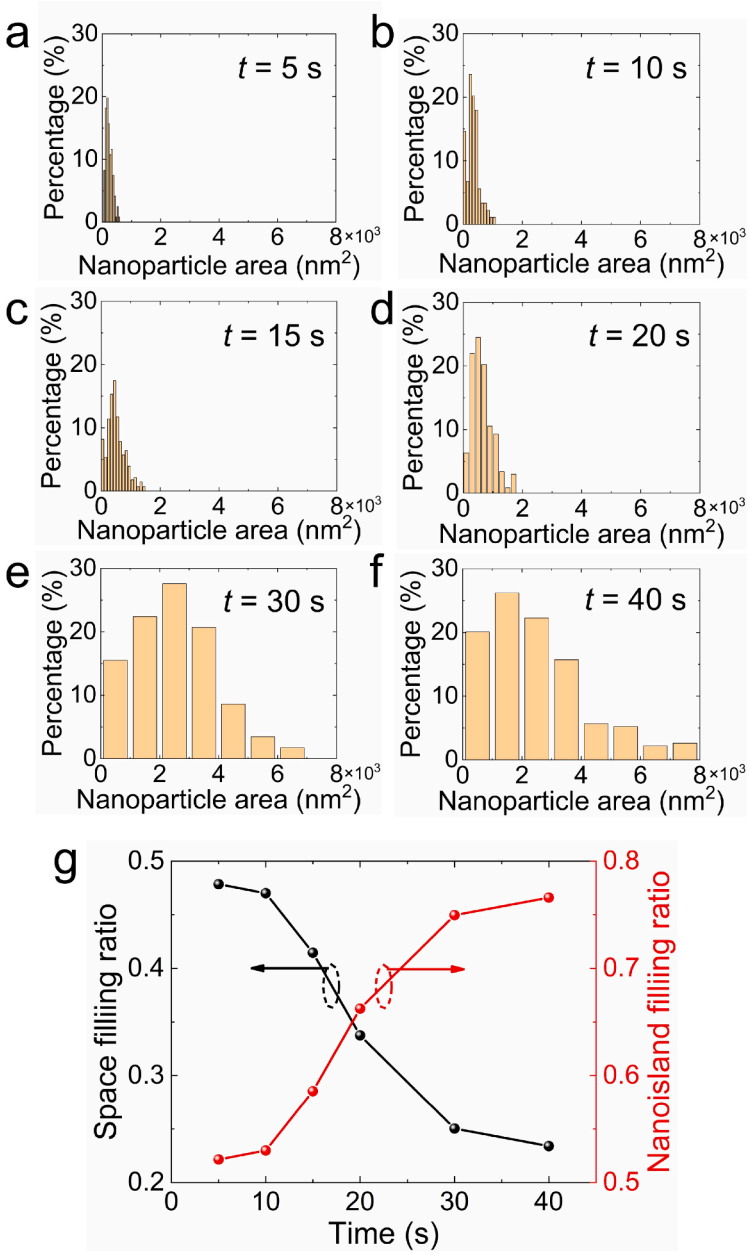

Fig. 2. Statistics of the size distribution of Au nanoislands obtained by using different sputtering times of (a) 10 s, (b) 15 s, (c) 20 s, (d) 25 s, (e) 30 s, and (f) 40 s. The evolution of the filling ratio of Au nanoislands (or space) with increasing sputtering time is shown in (g).

expect the existence of a large number of plasmonic hot spots in the gap regions between Au nanoislands. Therefore, it is expected that closely-packed Au nanoislands can produce efficient HEIL when being excited by femtosecond laser pulses.

We examined the HEIL emitted from Au nanoislands deposited at different sputtering times by using 800-nm femtosecond laser pulses, as shown in Fig. 3. We also compared the corresponding transmission spectra of these nanoislands (Figures S1, Supporting Information). For t = 10 s, Au nanoislands are well separated with large gaps (see Fig. 1a). In this case, only Au nanoislands with rod-like shapes can generate HEIL under the irradiation of the femtosecond laser pulses. As a result, very weak HEIL was observed at low laser fluences (F), as shown in Fig. 3a. An increase of HEIL was found when the laser fluence was raised from 0.16 to 0.31 mJ/cm^2. After that, the intensity of HEIL remains nearly unchanged when the laser fluence was increased from 0.62 to 1.55 mJ/cm^2, probably due to the melting of rod-like nanoislands which quenches the HEIL. For closely-packed Au nanoislands formed at t = 15 s, a dramatic increase in the HEIL by nearly one order of magnitude was observed, as shown in Fig. 3b. In this case, the efficient HEIL was ascribed to the formation of a large number of plasmonic hot spots in the gap regions between closely-packed Au nanoislands. Similarly, a slight reduction of the HEIL was seen when the laser fluence was raised from 1.24 to 1.55 mJ/cm^2, implying the disappearance of some plasmonic hot spots at high laser fluences. For closely-packed Au nanoislands obtained at t = 20 s, 25 s, 30 s, we observed quite similar behaviors in the laser fluence dependence of the HEIL intensity. A monotonic increase in the HEIL was observed when the laser fluence was increased, as shown in Fig. 3c,d,e. However, a further increase in the HEIL was found when the laser fluence was raised from 1.24 to 1.55 mJ/cm^2. It means that a larger laser fluence is needed in order to quench the plasmonic hot spots formed by the coupling of closely-packed Au nanoislands. For t = 30 s, a different behavior was observed. A relatively weaker HEIL was found at low laser fluences and it barely changed when the laser fluence was varied from 0.16 to 0.62 mJ/cm^2. From Fig. 1e, it is noticed that the

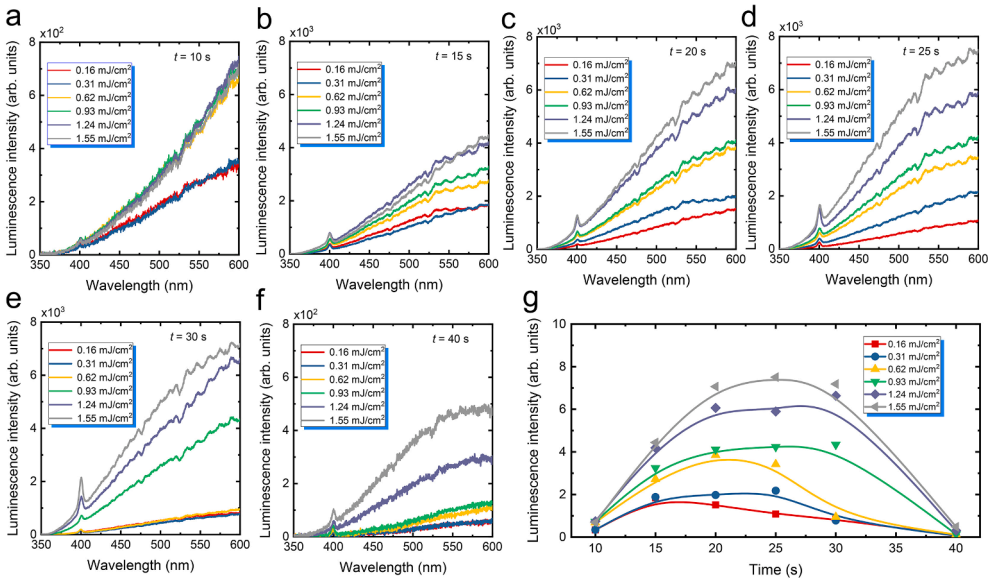

Fig. 3. Evolution of the luminescence spectra with increasing laser fluences measured for the closely-packed Au nanoislands deposited on SiO_2 substrates with different times of (a) 10 s, (b) 15 s, (c) 20 s, (d) 25 s, (e) 30 s, (f) 40 s. The dependences of the luminescence intensity on the excitation laser fluence measured for different samples are sumarized in (g).

sizes of Au nanoislands become larger and the gap widths between them become narrower. As a result, the SPRs of the plasmonic hot spots are shifted to longer wavelengths, leading to the reduction of the HEIL (Figures S1, Supporting Information). The irradiation of closely-packed Au nanoislands with femtosecond laser pulses with a small laser fluence results in the shrinkage of Au nanoislands, leading to the widening of the gap regions and the shift of the SPRs back to a shorter wavelength. Consequently, a rapid increase in the HEIL was observed at a laser fluence of 0.93 mJ/cm^2 and a further enhancement of the HEIL was found at laser fluences of 1.24 and 1.55 mJ/cm^2. For $t = 40$ s, the number of plasmonic hot spots with their SPRs appearing at $\sim$ 800 nm was reduced dramatically. Accordingly, a dramatic reduction of the HEIL was seen, as shown in Fig. 3f. The dependences of the HEIL intensity on the laser fluence measured for different samples are presented in Fig. 3g.

As mentioned above, a large number of plasmonic hot spots are expected to exist in closely-packed Au nanoislands. Significantly enhanced electric fields achieved at such hot spots lead to the emission of HEIL. Apparently, the appearance and location of hot spots exhibit a strong dependence on the polarization and wavelength of laser light [16–18]. This unique feature makes it possible to realize multi-dimensional optical data storage, which has been demonstrated in an assembly of Au nanorods [3,16]. Previously, a polymer film heavily doped with Au nanorods was employed as the medium for optical data storage. In this case, Au nanorods are supported by the mesh structure of the polymer film, which is not stable against the humidity of air and the heat released by Au nanorods. The latter may lead to the damage of the polymer film if the laser fluence used for data recording is large. It is highly desirable that Au nanorods can be doped in dielectric materials, such as silica or ceramic, so that the lifetime of the storage medium can reach several hundred years [19]. However, the achievement of such a data storage medium remains a big challenge from the viewpoint of fabrication technology. Here, we deposited closely-packed Au nanoislands on a SiO_2 substrate with the hope that a two-dimensional optical data storage medium, which is quite stable in the atmosphere, can be demonstrated.

In order to verify that optical data can be recorded and extracted by exploiting the HEIL emitted from the randomly distributed plasmonic hot spots in closely-packed Au nanoislands, we examined the changes in the HEIL spectrum of the sample with $t = 25$ s induced by irradiating femtosecond laser pulses with different laser fluences, as shown in Fig. 4a. In each case, the HEIL spectrum was obtained at a small laser

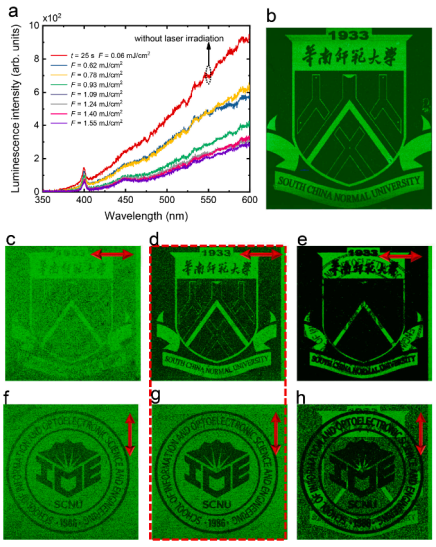

Fig. 4. (a) Comparison of the luminescence spectra of the Au/PVP film before and after the irradiation of femtosecond laser pulses with different fluences. (b) Image recorded and extracted in the sample with $t = 25$ s by using 800-nm femtosecond laser pulses. The images recorded by using 800–nm femtosecond laser pulses with cross polarizations (horizontally- and vertically polarized) and different laser fluences of 0.67, 0.75, 2.51 mJ/cm^2 and exracted by using femtosecond laser pulses with the same wavelength and polarization but a smaller laser fluence of 0.17 mJ/cm^2 are shown in (c)-(h), respectively. In each case, the polarization of the femtosecond laser light used for data recording and readout is indicated by an arrow.

fluence of 0.06 mJ/cm^2, which did not induce any change in the HEIL spectrum. As expected, the HEIL was found to be reduced by a factor of $\sim$ 3.0 after the irradiation of laser light with a large fluence (1.55 mJ/cm^2), which eliminates most hot spots in the area. Accordingly, an increase in the transmission of the sample at the laser wavelength (800 nm) was also observed because of eliminating hot spots at this wavelength (Figures S2, Supporting Information). We performed data recording and readout experiments by using a laser scanning confocal microscope, as shown in Fig. 4b where the logo of our university was

used. It is demonstrated that high-quality optical data storage, which is reflected in the large correlation coefficient and contrast of the extracted pattern (Figures S3, Supporting Information), can be realized by using closely-packed Au nanoislands. The correlation coefficient and contrast of the extracted image were estimated to be 0.96 and 0.66, both are better than those achieved in the storage medium made of a polymer doped with Au nanorods (Figures S4,S5 Supporting Information). In order to demonstrate the polarization multiplexing in optical data storage, we recorded two images (the university and school logos) in the same area of 100 × 100 μm^2 by using femtosecond laser pulses with cross polarizations (i.e., horizontally- and vertically-polarized). The images recorded by using three different fluences of 0.67, 0.75, 2.51 mJ/cm^2 and extracted by using femtosecond laser pulses with the same polarization and a smaller fluence (0.17 mJ/cm^2) are presented in Fig. 4c,d,e, respectively. For laser fluences smaller than 0.75 mJ/cm^2, no cross-talk was observed between the two recording channels, implying the realization of polarization multiplexing (see Fig. 4c,d). However, the quaility of the extracted image was not satisfied when a small laser fluence of 0.67 mJ/cm^2 was used, as shown in Fig. 4c. In contrast, cross-talk between the two recording channels appeared when a large laser fluence of 2.51 mJ/cm^2 was employed, although the image's contrast was improved simultaneously (see Fig. 4e). This result indicates that the optimum laser fluence for data recording with polarization multiplexing is found to be ∼ 0.75 mJ/cm^2. We also demonstrated that three polarization recording channels separated by 60° with negligible cross-talk can be realized by using closely-packed Au nanoislands. (Figures S6, Supporting Information).

Similarly, the wavelength-sensitive hot spots existing in the closely-packed Au nanoislands enable data recording with wavelength multiplexing. Owing to the spectral shift of the SPRs (Figures S2, Supporting Information), however, the small cross-talk between neighboring recording channels has not been completely removed (Figures S7, Supporting Information).

Very recently, it was found that highly localized temperature distribution can be achieved by exploiting the Fano resonances generated in the oligamers of Au nanoparticles [24]. The combination of the spatially localized temperature distribution and the catalytical function of Au nanoparticles can be utilized to produce carbon quantum dots with small diameters, which emit white light efficiently. Here, we showed that highly localized temperature distribution can also be achieved in two-dimensional closely-packed Au nanoparticles. Upon the irradiation of femtosecond laser pulses, reshaping of Au nanoislands appears, leading to the formation of closely-packed elliptical Au nanoparticles, as shown in Fig. 5a. The physical model we used to simulate the temperature distribution is also shown in Fig. 5a, where the nanoparticles selected from the SEM image were displayed in yellow color. Each nanoparticle was approximated as an ellipsoid with a similar volume. In order to reduce the burden of calculation, some nanoparticles with very small sizes were not included in the physical model. In Fig. 5b, we present the electric field distribution calculated for the physical model. Randomly distributed plasmonic hot spots, manifested themselves as significantly enhanced electric fields, can be identified in the electric field distribution. Based on the physical model shown in Fig. 5a, we also calculated the temperature distribution in the array of closely-packed Au nanoparticles. As an approximation, we simulated the temperature distribution in closely-packed Au nanoislands induced by a continuous wave laser beam by using a commercial software (see Method). The maximum temperature shown in Fig. 5c (∼ 370 K) is the temperature induced by a continuous wave laser beam with a diameter of 1.0 μm and a power of 1.0 mW (i.e., ∼ 0.16 mJ/cm^2). Here, it is important to reveal the formation of spatially localized "hot spots" which can be utilized to produce carbon quantum dots. A temperature much higher than 370 K can be achieved if we used a higher power laser beam. As can be seen in Fig. 5c, hot spots with highly-localized temperature distributions are created and they play a crucial role in the generation of carbon quantum dots [31–35], as demonstrated in the following.

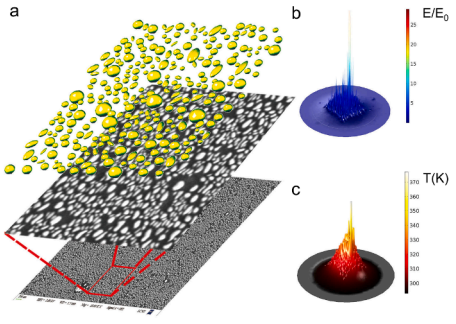

Fig. 5. (a) Au nanoparticles selected from the SEM image for numerical simulations. (b) Electric field distribution calculated for the assembly of Au nanoparticles at 800 nm. (c) Temperature distribution calculated for the same assemble of Au nanoparticles at 800 nm.

The existence of spatially-localized hot spots of temperature in closely-packed Au nanoparticles can be exploited to generate carbon quantum dots. In previous studies, carbon quantum dots were generated by exploiting the Fano resonances formed in the oligomers of Au nanoparticles appearing in the wavelength range of 600–650 nm [24]. No carbon quantum dots were obtained when 800 nm femtosecond laser pulses were used as the excitation source. Here, we showed that 800 nm femtosecond laser pulses from a Ti-saphire oscillator could be employed directly to produce carbon quantum dots from a polymer film spin-coated on top of two-dimensional closely-packed Au nanoparticles. In Fig. 6a, we present the school logo recorded in the sample consisting of a polymer (PVP) film and a metal film (i.e., two-dimensional closely-packed Au nanoparticles) by using 800-nm femtosecond laser pulses with recording and readout fluences of 3.82 and 0.17 mJ/cm^2. The large values of correlation coefficient and contrast, which were extracted to be 0.92 and 0.69 respectively, indicate the high quality of the recorded image. It can be seen that the area irradiated by femtosecond laser pulses with a large fluence appears to be dark due to the reduction of the HEIL. When we irradiated the image with a mercury lamp, the school logo was still visible, as shown in Fig. 6b. It is noticed, however, that the area irradiated by femtosecond laser pulses appears to be bright owing to the generation of carbon quantum dots that emit white light. The creation of carbon quantum dots was also confirmed in the image extracted by using a single-photon laser scanning confocal microscope, as shown in Fig. 6c. The image extracted by detecting the luminescence of the carbon quantum dots excited by a continuous wave laser also possesses a high quality. The above experiments also indicated that carbon quantum dots could not be lightened by using 800 nm femtosecond laser pulses.

Carbon quantum dots generated in this way can emit white light efficiently under the excitation of laser light at shorter wavelengths [36–41]. In Fig. 7, we show the images (the school logo) recorded in the above sample by using 800-nm femtosecond laser pulses and observed in the four wavelength channels of a single-photon laser scanning confocal microscope. The excitation wavelengths for the four images were 405, 488, 561, and 640 nm while the detection wavelength ranges of the four wavelength channels were 400–492 nm, 500–550 nm, 563–588 nm, and 601–657 nm, respectively. In this case, the image extracted by using 800 nm femtosecond laser light was similar to that shown in Fig. 4b

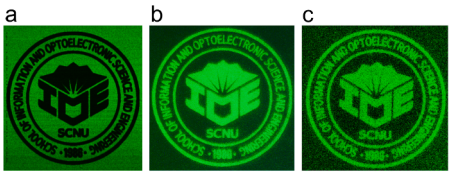

Fig. 6. Images recorded by using 800-nm femtosecond laser pulses and extracted by using (a) 800-nm femtosecond laser pulses, (b) mercury lamp and c) single-photon laser scanning confocal microscope.

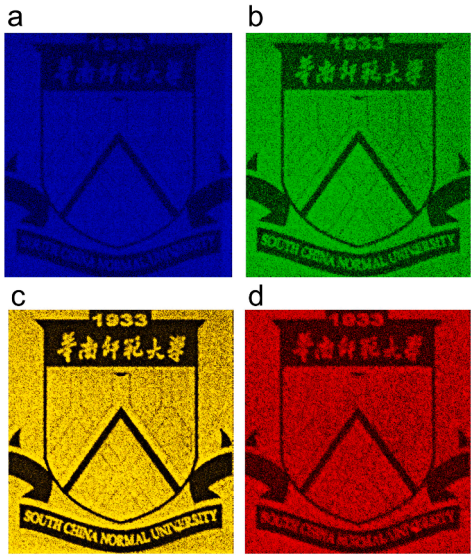

Fig. 7. Images recorded by using 800-nm femtosecond laser pulses and extracted by using a single-photon laser scanning confocal microscope with excitation wavelengths of (a) 405 nm, (b) 488 nm, (c) 561 nm, and (d) 640 nm. The corresponding wavelength ranges for collecting the luminescence are (a) 400–492 nm, (b) 500–550 nm, (c) 563–588 nm, and (d) 601–657 nm, respectively.

where the irradiated area appeared to be dark. In Fig. 7a-d, we can see clear images in all channels displayed by the light emitted from carbon quantum dots, which are complementary with that shown in Fig. 4b. It indicates that white light with broadband was generated when carbon quantum dots were excited by using laser light with a short wavelength. It is noticed, however, the clearest image is obtained in the yellow channel (563–588 nm), implying the peak position of the luminescence emitted from carbon quantum dots.

3. Concluding remarks

In summary, we proposed using two-dimensional close-packed Au nanoislands deposited on a SiO_2 substrate as the platform to realize simultaneously high-quality optical data storage with polarization multiplexing and highly efficient generation of carbon quantum dots. It was demonstrated numerically and experimentally that hot spots of both electric field and temperature, which are sensitive to the polarization and wavelength of laser light, can be created in closely-packed Au nanoparticles. It was shown that highly efficient HEIL can be genearted when closely-packed Au nanoparticles are excited by using femtosecond laser pulses and it can be exploited to realize optical data storage with high-quality and ultralow energy. It was revealed that carbon quantum dots can be generated in the polymer spin-coated on two-dimensional closely-packed Au nanoparticles by utilizing the hot spots of temperature and the catalytical properties of Au nanoparticles. Our findings indicate the potential applications of this new nanomaterial in the fabrication of novel photonic devices for optical data storage, optical display, and optical sensing in the future.

4. Method

Sample preparation: Two-dimensional Au nanoislands used in this work were deposited on SiO_2 substrates by sputtering. The morphology of the two-dimensional Au nanoislands could be modified by controlling the sputtering time and closely-packed Au nanoislands could be achieved by using a sputtering time larger than 10 s. Thin films of different polymers (PVA, PMMA and PVP) used for producing carbon quantum dots were spin-coated on the SiO_2 substrates with pre-deposited two-dimensional Au nanoislands. The thicknesses of the thin polymer films could be adjusted by varying the concentration of the polymer or the speed of spin-coating.

Experimental setup: The femtosecond laser light with a repetition rate of 76 MHz and a duration of 130 fs (Mira 900S, Coherent) was employed for optical data storage and carbon dot generation. It was focused on the samples by using the 60× objective lens (NA = 0.85) of a two-photon laser scanning confocal microscope (A1MP, Nikon) or a inverted luminescence microscope (Obsever A1, Zeiss). The generated optical signals (i.e., HEIL of Au nanoparticles) were collected by using the same objective lens and directed to the spectrometer attached to the microscope for analysis. The HEIL of Au nanoparticles in the wavelength range of 450–650 nm was detected. Data recording and readout were completed by using the raster scanning system of the microscope. The extraction of the patterns composed of carbon quantum dots induced by femtosecond laser pulses was realized by using a single-photon laser scanning confocal microscope (A1, Nikon).

Numerical modeling: The electric field distributions in two-dimensional closely-packed Au nanoislands and the temperature distributions in two-dimensional arrays of Au nanoparticles were calculated numerically based on the finite element method (FEM) by using a commercially developed software (COMSOL Multiphysics v5.4). A perfectly matched layer boundary condition was employed to ensure the absorption of all the outgoing radiations. The temperature inside each Au nanoparticle was assumed to be uniform owing to the small size of nanoparticles and good conductivity of Au.

5. Front matter

The author names and affiliations could be formatted in two ways:

(1) Group the authors per affiliation.
(2) Use footnotes to indicate the affiliations.

See the front matter of this document for examples. You are recommended to conform your choice to the journal you are submitting to.

Declaration of Competing Interest

The authors declare that they have no known competing financial interests or personal relationships that could have appeared to influence the work reported in this paper.

Acknowledgments

S. Lan and S. Tie acknowledge the financial support from the National Key Research and Development Program of China (No. 2016YFA0201002), the National Natural Science Foundation of China (Grant Nos. 11674110 and 11874020), and the Natural Science Foundation of Guangdong Province, China (Grant No. 2016A030308010). Y. Xu acknowledges the financial support from the National Natural Science Foundation of China (Nos. 91750110, 11674130), the Natural Science Foundation of Guangdong Province (Nos. 2016A030306016, 2016TQ03X981), and Pearl River S and T Nova Program of Guangzhou (No. 201806010040).

Appendix A. Supplementary material

Supplementary data associated with this article can be found, in the online version, at https://doi.org/10.1016/j.apsusc.2021.149586.

References

[1] J.N. Anker, W.P. Hall, O. Lyandres, N.C. Shah, J. Zhao, R.P. Van Duyne, Biosensing with plasmonic nanosensors, Nat. Mater. 7 (2008) 442–453.
[2] P. Zijlstra, M. Orrit, Single metal nanoparticles: optical detection, spectroscopy and applications, Rep. Prog. Phys. 74 (2011) 106401.

[3] P. Zijlstra, J.W.M. Chon, M. Gu, Five-dimensional optical recording mediated by surface plasmons in gold nanorods, Nature 459 (2009) 410–413.
[4] F. Hao, Y. Sonnefraud, P. Van Dorpe, S.A. Maier, N.J. Halas, P. Nordlander, Symmetry Breaking in Plasmonic Nanocavities: Subradiant LSPR Sensing and a Tunable Fano Resonance, Nano Lett. 8 (2008) 3983–3988.
[5] Z. Fang, X. Zhu, Plasmonics in Nanostructures, Adv. Mater. 25 (2013) 3840–3856.
[6] J. Olson, A. Manjavacas, L.F. Liu, W.S. Chang, B. Foerster, N.S. King, M.W. Knight, P. Nordlander, N.J. Halas, S. Link, Vivid, full-color aluminum plasmonic pixels, Proc. Natl. Acad. Sci. U.S.A. 111 (2014) 14348–14353.
[7] H.R. Ren, X.P. Li, Q.M. Zhang, M. Gu, On-chip noninterference angular momentum multiplexing of broadband light, Science 352 (2016) 805–809.
[8] R.F. Oulton, V.J. Sorger, T. Zentgraf, R.-M. Ma, C. Gladden, L. Dai, G. Bartal, X. Zhang, Plasmon lasers at deep subwavelength scale, Nature 461 (2009) 629–632.
[9] K. Saha, S.S. Agasti, C. Kim, X. Li, V.M. Rotello, Gold Nanoparticles in Chemical and Biological Sensing, Chem. Rev. 112 (2012) 2739–2779.
[10] J.D. Chen, J. Xiang, S. Jiang, Q.F. Dai, S.L. Tie, S. Lan, Radiation of the high-order plasmonic modes of large gold nanospheres excited by surface plasmon polaritons, Nanoscale 10 (2018) 9153–9163.
[11] X.X. Chen, Y.Q. Yang, Y.H. Chen, M. Qiu, R.J. Blaikie, B.Y. Ding, Probing Plasmonic Gap Resonances between Gold Nanorods and a Metallic Surface, J. Phys. Chem. C 119 (2015) 18627–18634.
[12] P. Zijlstra, J.W.M. Chon, M. Gu, Effect of heat accumulation on the dynamic range of a gold nanorod doped polymer nanocomposite for optical laser writing and patterning, Opt. Exp. 15 (2007) 12151–12160.
[13] T. Li, Q. Li, Y. Xu, X.J. Chen, Q.F. Dai, H.Y. Liu, S. Lan, S.L. Tie, L.J. Wu, Three-Dimensional Orientation Sensors by Defocused Imaging of Gold Nanorods through an Ordinary Wide-Field Microscope, ACS nano 6 (2012) 1268–1277.
[14] Y.Q. Jiang, N.N. Horimoto, K. Imura, H. Okamoto, K. Matsui, R. Shigemoto, Bioimaging with Two-Photon-Induced Luminescence from Triangular Nanoplates and Nanoparticle Aggregates of Gold, Adv. Mater. 21 (2009) 2309–2313.
[15] Z.M. Chen, H.H. Fan, J.X. Li, S.L. Tie, S. Lan, Photothermal therapy of single cancer cells mediated by naturally created gold nanorod clusters, Opt. Exp. 25 (2017) 15093–15107.
[16] Q. Dai, M. Ouyang, W. Yuan, J. Li, B. Guo, S. Lan, S. Liu, Q. Zhang, G. Lu, S. Tie, H. Deng, Y. Xu, M. Gu, Encoding Random Hot Spots of a Volume Gold Nanorod Assembly for Ultralow Energy Memory, Adv. Mater. 29 (2017) 1701918.
[17] Y. Zheng, H. Liu, J. Xiang, Q. Dai, M. Ouyang, S. Tie, S. Lan, Hot luminescence from gold nanoflowers and its application in high-density optical data storage, Opt. Exp. 25 (2017) 9262–9275.
[18] Y.H. Chu, H.M. Xiao, G. Wang, J. Xiang, H.H. Fan, H.Y. Liu, Z.C. Wei, S.L. Tie, S. Lan, Q.F. Dai, Randomly Distributed Plasmonic Hot Spots for Multilevel Optical Storage, J. Phys. Chem. C 122 (2018) 15652–15658.
[19] Q.M. Zhang, Z.L. Xia, Y.B. Cheng, M. Gu, High-capacity optical long data memory based on enhanced Young's modulus in nanoplasmonic hybrid glass composites, Nat. Commun. 9 (2018) 1–6.
[20] T. Haug, P. Klemm, S. Bange, J.M. Lupton, Hot-electron intraband luminescence from single hot Spots in noble-metal nanoparticle films, Phys. Rev. Lett. 115 (2015) 067403.
[21] L. Roloff, P. Klemm, I. Gronwald, R. Huber, J.M. Lupton, S. Bange, Light Emission from Gold Nanoparticles under Ultrafast Near-Infrared Excitation: Thermal Radiation, Inelastic Light Scattering, or Multiphoton Luminescence? Nano Lett. 17 (2017) 7914–7919.
[22] J. Xiang, S. Jiang, J. Chen, J. Li, Q. Dai, C. Zhang, Y. Xu, S. Tie, S. Lan, Hot-electron intraband luminescence from GaAs nanospheres mediated by magnetic dipole resonances, Nano Lett. 17 (2017) 4853–4859.
[23] J. Mertens, M.-E. Kleemann, R. Chikkaraddy, P. Narang, J.J. Baumberg, How Light Is Emitted by Plasmonic Metals, Nano Lett. 17 (2017) 2568–2574.
[24] Y.B. Zheng, H.Y. Liu, J.X. Li, J. Xiang, M.C. Panmai, Q.F. Dai, Y. Xu, S.L. Tie, S. Lan, Controllable Formation of Luminescent Carbon Quantum Dots Mediated by the Fano Resonances Formed in Oligomers of Gold Nanoparticles, Adv. Mater. 31 (2019) 1901371.
[25] S.Y. Lim, W. Shen, Z.Q. Gao, Carbon quantum dots and their applications, Chem. Soc. Rev. 44 (2015) 362–381.
[26] H. Li, Z. Kang, Y. Liu, S.-T. Lee, Carbon nanodots: synthesis, properties and applications, J. Mater. Chem. 22 (2012) 24230–24253.
[27] F.L. Yuan, Z.B. Wang, X.H. Li, Y.C. Li, Z.A. Tan, L.Z. Fan, S.H. Yang, Bright Multicolor Bandgap Fluorescent Carbon Quantum Dots for Electroluminescent Light-Emitting Diodes, Adv. Mater. 29 (2017) 1604436.
[28] Z.F. Wang, F.L. Yuan, X.H. Li, Y.C. Li, H.Z. Zhong, L.Z. Fan, S.H. Yang, 53% Efficient Red Emissive Carbon Quantum Dots for High Color Rendering and Stable Warm White-Light-Emitting Diodes, Adv. Mater. 29 (2017) 1702910.
[29] H. Ding, S.B. Yu, J.S. Wei, H.M. Xiong, Full-Color Light-Emitting Carbon Dots with a Surface-State-Controlled Luminescence Mechanism, ACS nano 10 (2016) 484–491.
[30] S. Sheikholeslami, Y.W. Jun, P.K. Jain, A.P. Alivisatos, Coupling of Optical Resonances in a Compositionally Asymmetric Plasmonic Nanoparticle Dimer, Nano Lett. 10 (2010) 2655–2660.
[31] L.A. Zhou, D.F. Swearer, C. Zhang, H. Robatjazi, H.Q. Zhao, L. Henderson, L. L. Dong, P. Christopher, E.A. Carter, P. Nordlander, N.J. Halas, Quantifying hot carrier and thermal contributions in plasmonic photocatalysis, Science 362 (2018) 69–72.
[32] X.P. Tao, Y.Y. Gao, S.Y. Wang, X.Y. Wang, Y. Liu, Y. Zhao, F.T. Fan, M. Dupuis, R. G. Li, C. Li, Interfacial Charge Modulation: An Efficient Strategy for Boosting Spatial Charge Separation on Semiconductor Photocatalysts, Adv. Energy Mater. 9 (2019) 1803951.
[33] D.F. Swearer, H.Q. Zhao, L.N. Zhou, C. Zhang, H. Robatjazi, J.M.P. Martirez, C. M. Krauter, S. Yazdi, M.J. McClain, E. Ringe, E.A. Carter, P. Nordlander, N.J. Halas, Heterometallic antenna-reactor complexes for photocatalysis, Proc. Natl. Acad. Sci. U.S.A. 113 (2016) 8916–8920.
[34] B. Foerster, A. Joplin, K. Kaefer, S. Celiksoy, S. Link, C. Sonnichsen, Chemical Interface Damping Depends on Electrons Reaching the Surface, ACS nano 11 (2017) 2886–2893.
[35] P. Christopher, H.L. Xin, A. Marimuthu, S. Linic, Singular characteristics and unique chemical bond activation mechanisms of photocatalytic reactions on plasmonic nanostructures, Nat. Mater. 11 (2012) 1044–1050.
[36] X. Miao, D. Qu, D.X. Yang, B. Nie, Y.K. Zhao, H.Y. Fan, Z.C. Sun, Synthesis of Carbon Dots with Multiple Color Emission by Controlled Graphitization and Surface Functionalization, Adv. Mater. 30 (2018) 1704740.
[37] J.C. Liu, N. Wang, Y. Yu, Y. Yan, H.Y. Zhang, J.Y. Li, J.H. Yu, Carbon dots in zeolites: A new class of thermally activated delayed fluorescence materials with ultralong lifetimes, Sci. Adv. 3 (2017) e1603171.
[38] Z.C. Jiang, T.N. Lin, H.T. Lin, M.J. Talite, T.T. Tzeng, C.L. Hsu, K.P. Chiu, C.A. J. Lin, J.L. Shen, C.T. Yuan, A Facile and Low-Cost Method to Enhance the Internal Quantum Yield and External Light-Extraction Efficiency for Flexible Light-Emitting Carbon-Dot Films, Sci. Rep. 6 (2016) 19991.
[39] Q.Q. Fang, Y.Q. Dong, Y.M. Chen, C.H. Lu, Y.W. Chi, H.H. Yang, T. Yu, Luminescence origin of carbon based dots obtained from citric acid and amino group-containing molecules, Carbon 118 (2017) 319–326.
[40] Y.H. Deng, X. Chen, F. Wang, X.A. Zhang, D.X. Zhao, D.Z. Shen, Environment-dependent photon emission from solid state carbon dots and its mechanism, Nanoscale 6 (2014) 10388–10393.
[41] Q.J. Li, M. Zhou, Q.F. Yang, Q. Wu, J. Shi, A.H. Gong, M.Y. Yang, Efficient Room-Temperature Phosphorescence from Nitrogen-Doped Carbon Dots in Composite Matrices, Chem. Mater. 28 (2016) 8221–8227.